

# REPORT DOCUMENTATION PAGE

Form Approved  
OMB No. 0704-0188

Public reporting burden for this collection of information is estimated to average 1 hour per response, including the time for reviewing instructions, searching existing data sources, gathering and maintaining the data needed, and completing and reviewing this collection of information. Send comments regarding this burden estimate or any other aspect of this collection of information, including suggestions for reducing this burden to Department of Defense, Washington Headquarters Services, Directorate for Information Operations and Reports (0704-0188), 1215 Jefferson Davis Highway, Suite 1204, Arlington, VA 22202-4302. Respondents should be aware that notwithstanding any other provision of law, no person shall be subject to any penalty for failing to comply with a collection of information if it does not display a currently valid OMB control number. PLEASE DO NOT RETURN YOUR FORM TO THE ABOVE ADDRESS.

1. REPORT DATE (DD-MM-YYYY) 2. REPORT TYPE Technical Papers 3. DATES COVERED (From - To)

4. TITLE AND SUBTITLE 5a. CONTRACT NUMBER 5b. GRANT NUMBER 5c. PROGRAM ELEMENT NUMBER

6. AUTHOR(S) Please see attached 5d. PROJECT NUMBER 2302 5e. TASK NUMBER M1G2 5f. WORK UNIT NUMBER 346120

7. PERFORMING ORGANIZATION NAME(S) AND ADDRESS(ES) Air Force Research Laboratory (AFMC) AFRL/PRS 5 Pollux Drive Edwards AFB CA 93524-7048 8. PERFORMING ORGANIZATION REPORT

9. SPONSORING / MONITORING AGENCY NAME(S) AND ADDRESS(ES) Air Force Research Laboratory (AFMC) AFRL/PRS 5 Pollux Drive Edwards AFB CA 93524-7048 10. SPONSOR/MONITOR'S ACRONYM(S) 11. SPONSOR/MONITOR'S NUMBER(S) Please see attached

12. DISTRIBUTION / AVAILABILITY STATEMENT Approved for public release; distribution unlimited.

13. SUPPLEMENTARY NOTES

14. ABSTRACT 20030129 198

15. SUBJECT TERMS

16. SECURITY CLASSIFICATION OF:			17. LIMITATION OF ABSTRACT A	18. NUMBER OF PAGES	19a. NAME OF RESPONSIBLE PERSON Leilani Richardson
a. REPORT Unclassified	b. ABSTRACT Unclassified	c. THIS PAGE Unclassified			19b. TELEPHONE NUMBER (include area code) (661) 275-5015

2302P11

G2

MEMORANDUM FOR PRR (In-House Publication)

FROM: PROI (TI) (STINFO)

01 Aug 2000

SUBJECT: Authorization for Release of Technical Information, Control Number: **AFRL-PR-ED-TP-2000-157**  
Liu, C.T. (AFRL/PRSM), "Observation of Damage Process in a Particulate Composite Material by Real-Time Radiographic Techniques"

**Journal of Nondestructive Testing and Evaluation**  
**(Submission Deadline: 07 Aug 00)**

**(Statement A)**

1. This request has been reviewed by the Foreign Disclosure Office for: a.) appropriateness of distribution statement, b.) military/national critical technology, c.) export controls or distribution restrictions, d.) appropriateness for release to a foreign nation, and e.) technical sensitivity and/or economic sensitivity.

Comments: \_\_\_\_\_  
\_\_\_\_\_  
\_\_\_\_\_

Signature \_\_\_\_\_ Date \_\_\_\_\_

2. This request has been reviewed by the Public Affairs Office for: a.) appropriateness for public release and/or b) possible higher headquarters review.

Comments: \_\_\_\_\_  
\_\_\_\_\_  
\_\_\_\_\_

Signature \_\_\_\_\_ Date \_\_\_\_\_

3. This request has been reviewed by the STINFO for: a.) changes if approved as amended, b.) appropriateness of distribution statement, c.) military/national critical technology, d.) economic sensitivity, e.) parallel review completed if required, and f.) format and completion of meeting clearance form if required

Comments: \_\_\_\_\_  
\_\_\_\_\_  
\_\_\_\_\_

Signature \_\_\_\_\_ Date \_\_\_\_\_

4. This request has been reviewed by PR for: a.) technical accuracy, b.) appropriateness for audience, c.) appropriateness of distribution statement, d.) technical sensitivity and economic sensitivity, e.) military/national critical technology, and f.) data rights and patentability

Comments: \_\_\_\_\_  
\_\_\_\_\_

APPROVED/APPROVED AS AMENDED/DISAPPROVED

\_\_\_\_\_  
LAWRENCE P. QUINN  
Technical Advisor  
Rocket Propulsion Division

\_\_\_\_\_  
DATE

# Observation of Damage Process in a Particulate Composite Material by Real-Time Radiographic Techniques

C. T. Liu  
Air Force Research Laboratory  
AFRL/PRSM  
10 E. Saturn Blvd.  
Edwards AFB CA 93524-7680

## Abstract

The damage initiation and evolution processes in pre-cracked sheet specimens subjected to different loading conditions, constant strain rate and constant strain, were investigated using real-time x-ray techniques. The specimens were made of a particulate composite material containing hard particles embedded in a rubber matrix. The x-ray data were analyzed and the results are discussed.

## Introduction

It is well known that a highly filled particulate composite material, on the microscopic scale, can be considered a nonhomogeneous material. Depending upon the degree of crosslink of the matrix material, filler particle size and distribution, and the bond strength at the interface of the particle and the matrix, the local stress and strength will vary in a random fashion. Therefore, when the material is strained, damage may develop in the material. The damage developed in the material may be in the form of microcracks or microvoids in the matrix or in the form of dewetting between the particle and the matrix. The damage will not be confined to a specific location; rather, it will diffuse into a relatively large area or zone. The growth of damage in the material may take place by tearing of the material or by successive nucleation and coalescence of the microvoids. The importance of study on damage initiation and evolution stems from the fact that damage can significantly affect the constitutive and the crack growth behavior in these materials. It is known that, throughout the loading history, the progressive development and interaction of various damage modes change the state of the material and the response of the structures. In addition to the micro-damage, large cracks can also develop in the material either during the manufacturing processes or by service loads. Therefore, to effectively use the material in structural applications one needs to understand the damage initiation and evolution processes, the effects of damage and crack development on the material's response, and the remaining strength and life of the structures.

In past years, a considerable amount of effort was spent in obtaining a fundamental understanding of damage initiation and its evolutionary process as well as the effects of damage on the material's constitutive and crack growth behavior in a highly filled polymeric material (Refs.1-5). Much of what we know about the damage process under different loading conditions has been obtained using nondestructive testing techniques. During the course of the damage studies, different nondestructive testing techniques were used. Experimental findings reveal that damage, expressed in terms of the attenuation of the acoustic energy, increases with increasing strain rate and the critical damage is relatively insensitive to the strain rate. They also reveal that the damage state correlates well with the

constitutive behavior of the material. The ultrasonic technique used in this study can be used to monitor damage initiation and evolution processes in a small region of the material. In order to determine the damage field in a large area, acoustic-imaging technique was used. By using the acoustic imaging technique, the damage characteristics near the crack tip are determined. The acoustic imaging data show that, due to the viscoelastic nature of the materials, load history and time have a significant effect on the damage characteristics in the materials.

In this study, the damage fields near the crack tip in edge-cracked sheet specimens subjected to a constant strain rate of  $1.0 \text{ min}^{-1}$  and a constant strain of 13% were investigated using real-time radiograph techniques. During the tests, Lockheed-Martin Research Laboratory's high-energy real-time x-ray system (HERTS) was used to monitor damage initiation and evolution processes near the crack tip. The experimental data were analyzed and the results are discussed.

### The experiments

The damage field near the crack tip in edged-cracked and centrally cracked sheet specimens subjected to a constant strain rate of  $1.0 \text{ min}^{-1}$  and a constant strain of 13% were investigated using real-time x-ray techniques. The specimens were made of a particulate composite material, containing hard particles embedded in a rubbery matrix. For the edged-cracked specimen and the centrally cracked specimen, prior to testing, a 23-mm crack was cut at the edge and the center of the specimens with a razor blade, respectively. The specimen geometries are shown in Figure 1. During the test, Lockheed-Martin Research Laboratory's HERTS was used to investigate the characteristics of the damage field near the crack tip. The specimen was placed between the x-ray radiation source and the x-ray camera. The x-ray image exits from the specimen and strikes the screen that is in front of the x-ray camera. The screen converts the x-ray image into a light image. This image is reflected into a low-light-level television camera by a mirror placed at  $45^\circ$  to the beam in the back of the camera. This isocon TV camera then converts the light image into an electronic signal that can be routed into the main monitor and into the video tape recorder. A detailed description of the HERTS system can be found in Reference 6. The recorded x-ray data were processed to create a visual indication of the energy absorbed in the material. A region of high absorption (i.e., a low damage area) will be shown as a dark area, whereas a region of low absorption will produce a light or white area, with 254 shades of gray in between. Also, the x-ray image at a given applied strain level can be plotted in the form of iso-intensity contours of the transmitted x-ray energy to enhance the resolution of the damaged field.

### Results and discussion

For a highly filled polymeric material that consists of a large number of fine particles, on the microscopic scale, it can be considered nonhomogeneous. When this material is stretched, the different sizes and distribution of the filler particles, the different crosslinking density of the polymer chains, and the variation of the bond strength between the particles and the binder can produce highly nonhomogeneous local stress and strength fields. Because of the particle's high rigidity relative to the binder, the local stress is significantly higher than that of the applied stress, especially when the particles are close to each other. Since local stress and strength vary in a random fashion, the failure site in the material also varies randomly and does not necessarily coincide with the maximum stress location. In other words, the location and degree of damage will also vary randomly in the material.

The damage may appear in the form of microcracks and microvoids in the binder, or in the form of particle/binder separation known as dewetting. When the particle is dewetted, the local stress will be redistributed. With time, additional particle/binder separation and vacuole formation takes place. This time-dependent process of dewetting nucleation, or damage nucleation, is due to the time-dependent processes of stress redistribution and particle/binder separation. Depending on the formation of the material and testing condition, damage growth may take place as material tearing or by successive nucleation and coalescence of the microvoids. These damage initiation and evolution processes are time-dependent, and are the main factor responsible for the time-sensitivity of the strength degradation as well as the fracture behavior of the material.

When crack occurs, the high stress at the crack tip will induce high damage near the crack tip region. The high damage zone at the crack tip is defined as the failure process zone that is a key parameter in viscoelastic fracture mechanics (Refs.7 and 8). Experimental data reveal that when the local strain reaches a critical value, small voids are generated in the failure process zone. Due to the random nature of the microstructure, the first void is not necessarily formed in the immediate neighborhood of the crack tip. The formation of the voids is not restricted to the surface of the specimen where the maximum normal strain occurs. Since the tendency of the filler particle to separate from the binder under a triaxial loading condition is high, it is expected that voids, or damage zone, will also be generated in the specimen's interior. Consequently, there are a large number of strands, which separate the voids and are essentially made of the binder material, that form inside the failure process zone as shown in Figure 2. Under this condition, the transverse constraint is minimized. As the applied strain increases with time, material fracture would occur at the blunted end of the crack tip. The failure of the material between the void and the crack tip leads the crack to grow a short distance. In other words, the coalescence of the void and the crack tip leads the crack to grow into the failure process zone. This kind of crack growth mechanism continues until the main crack tip reaches the failure process zone tip. When this occurs, the crack tip resharpen temporarily.

The above paragraph discussed the damage mechanisms in the particle-filled polymeric material. In order to determine the damage intensity and the damage fields near the tip of the propagating crack, real-time x-ray test data were analyzed. The results of the analyses are discussed in the following paragraphs.

Figure 3 shows the contours of transmitted x-ray energy near the tip of a propagating crack under the constant strain rate condition. In this figure, the number between two contour lines is the minimum intensity level of a range of  $I_t$  between the minimum intensity level and the next intensity level. A small number indicates that the intensity of the transmitted x-ray energy is high or that the damage is high. These contour plots show the details of the size and shape of the damage zone as well as the damage intensity inside the damage zone. As seen in Figure 3, the size of the damage zone and the intensity of damage in the damage zone increase with increasing applied strain level, and the damage gradient near the crack tip is very steep. The region that has a steep damage gradient is restricted to a very small area in the immediate neighborhood of the crack tip. When the applied strain level is low, the damage intensity outside the steep damage gradient area is negligible. As the applied strain level is increased, the damage gradient is decreased and the size of the highly damaged region is increased as shown in Figure 3. These experimental findings, obtained from real-time x-ray data, are consistent with experimental findings reported by Smith et al. (Ref.9) in their study of local strain distribution

near the crack tip in a highly filled polymeric material. As pointed out by Smith, the intense strain zone, or the highly strained region, ahead of the crack tip is very small and the strain level outside the intense strain is approximately equal to the applied strain level. A typical plot of the iso-strain contours near the crack tip is shown in Figure 4. By comparing Figure 4 with Figures 3 and 6, we note that the iso-intensity contours of  $I_t$ , or the shape of the damage zones, are similar to the iso-strain contours. This implies that the damage distribution is roughly commensurate with the strain distribution. Since the x-ray measures the average damage distribution through the thickness of the specimen, the similarity between the iso-intensity contours and the iso-strain contours implies that the surface strain measurement does roughly represent the strain distribution through the thickness of the specimen. However, it should be pointed out that the complex damage processes in the material depend on time, load history, and the microstructure of the material. Therefore, the roles that these parameters play on the complex phenomenon of damage initiation and evolution processes are not clear and additional work needs to continue.

Plot of crack growth rate versus time is shown in Figure 5. Figure 5 reveals that a pronounced fluctuation of crack growth velocity occurs during the entire time of crack growth. In other words, the crack growth process consists of a slow-fast-slow phenomenon. As mentioned earlier, the damage process is a time-dependent process and it required some time to develop a failure process zone at the crack tip. Thus, the crack growth process consists of blunt-growth-blunt and slow-fast-slow phenomena, which is highly nonlinear.

In the above paragraph, we discussed the damage field near the crack tip and the crack growth behavior when the specimen is subjected to the constant strain rate condition. In the following paragraph, we will discuss the damage field near the crack tip when the specimen is subjected to a constant strain condition.

Figure 6 shows the damage characteristics near the tip of the propagating crack when the specimen was held at a constant strain. From Figure 6, we see that the crack tip is relatively sharp and two small damage zones with high damage intensities,  $I_t$  equal to 40 and 50, developed. As time elapses, the crack tip become blunted and the damage intensity near the crack tip is increased and the damage intensities  $I_t$  in the two highly damaged regions increase from 50 and 40 to 30 (Figure 6). As the crack grows a short distance, the damage intensity near the crack tip increases further, and, a void is formed in the region where  $I_t$  equal to 20. Finally, the main crack tip and the void are joined, leading to the fracture of the specimen.

It is known that the damage characteristics near the crack tip are directly related to the stress states, which, in turn, is related to the crack tip geometry. In order to see how the crack tip geometry affect the damage field near the crack tip, an experiment was conducted on a specimen with a blunted crack tip. The experimental results are discussed in the following paragraph.

Figure 7 show the iso-intensity contours near the right-side tip of the crack at different applied strain levels. From this figure, it is seen that the crack tip is highly blunted. Under this condition, the high stress region changes from the crack tip to the upper and the lower corners of the blunted crack tip. Consequently, the high damage fields also shift to the corners of the blunted crack tip. When the applied strain level is increased from 3% to 6%, two small regions with relatively high damage



intensity are developed at small distances away from the corners of the blunted crack tip. With increasing applied strain level, voids are developed in the highly damaged regions. This indicates that the damage initiation and evolution processes are closely related to the crack tip geometry and the local microstructure.

## Conclusions

The damage characteristics near the crack tip in a particulate composite material subjected to a constant strain rate were investigated using real-time x-ray techniques. Experimental findings reveal that damage zone size and the intensity of damage inside the damage zone increase with increasing time, and the pre-damage does affect the crack growth behavior in the material. It also reveals the real-time x-ray technique is a promising technique to monitor damage initiation and evolution processes in the particulate composite material.

Reliable performance of a structure in critical applications depends on assuring that the structure in service satisfies the conditions assumed in design and life prediction analyses. Reliability assurance requires the availability of nondestructive evaluation (NDE) techniques not only for defect detection but also for verification of mechanical strength and associated properties. Therefore, NDE should not be defined solely by the current emphasis on the detection of overt flaws. Certainly it is necessary to extend NDE technology to characterize discrete flaws according to their location, size, orientation, and nature. This leads to an improved assessment of the potential criticality of individual flaws. Concurrently, it is necessary to extend NDE techniques for characterizing various material properties. In this case, the emphasis is on evaluation of microstructural and morphological factors that ultimately govern the material's strength and performance.

## References

- (1) Liu, C. T., "Evaluation of Damage Fields near Crack Tip in a Composite Solid Propellant," *Journal of Spacecrafts and Rockets*, Vol. 28, No. 1, pp 64-70, 1991.
- (2) Liu, C. T., "Acoustic Evaluation of Damage Characteristics in a Composite Solid Propellant," *Journal of Spacecrafts and Rockets*, Vol. 29, No. 5, pp 709-712, 1992.
- (3) Tang, B., Liu, C.T. and Henneke, E.G., "Acoustic-Ultrasonic Technique Applied to the Assessment of Damage in a Particulate Composite," *Journal of Spacecraft and Rockets*, Vol. 32, No. 5, 1995.
- (4) Liu, C. T. and Ravi-Chandran K., "Local Fracture and Crack Growth in a Particulate Composite Material," *Journal of Reinforced Plastic and Composites*, Vol. 36, No. 3, pp 196-207, 1996.
- (5) Liu, C. T. and Smith, C. W., "Temperature and Rate Effects on Stable Crack Growth in a Particulate Composite Material," *Experimental Mechanics*, Vol. 36, No. 3, pp 290-295, 1996.
- (6) Skelnsky, A. F. and Buchanan R., "Sensitivity of High-Energy Real-Time Radiography with Digital Integration," ASTM STP 716, pp 315-329, 1985.
- (7) Schapery, R. A., "A Theory of Crack Initiation and Growth in Viscoelastic Media," *Int. Journal of Fracture Mechanics*, Vol. 11, pp 141-159, 1975.
- (8) Knauss, W.G., "Delayed Failure - The Griffith Problem for Linearly Viscoelastic Materials," *International Journal of Fracture Mechanics*, Vol. 6, pp 7-20, March 1970.

- (9) Smith, C. W. and Liu, C. T., " Effects of near Tip Behavior of Particulate Composites on Classical Fracture Concepts," Journal of Composites and Engineering, Vol. 1. pp 249-256, 1991.



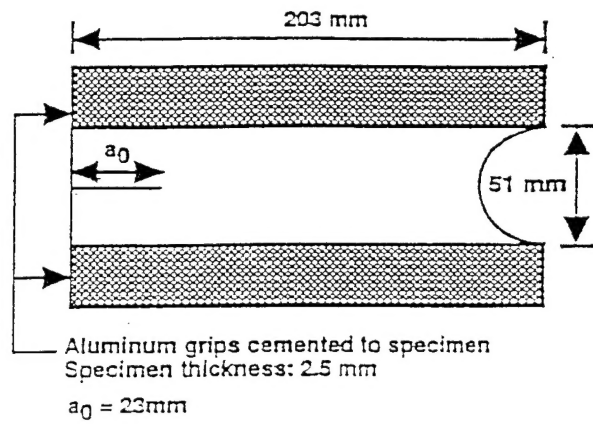
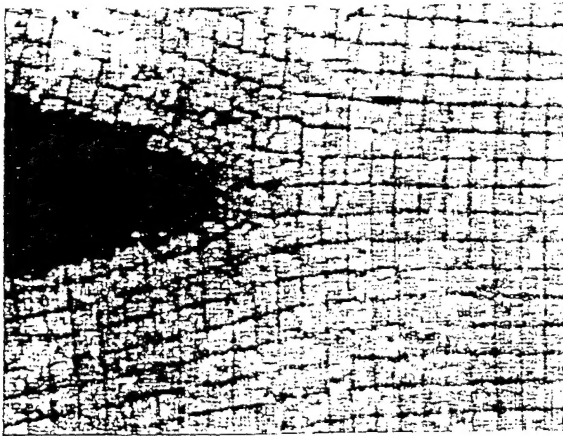
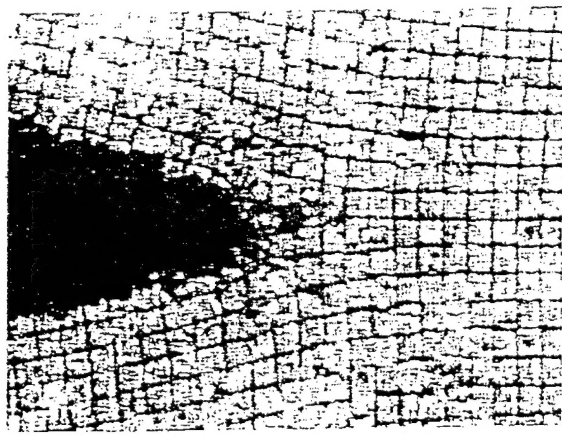


Figure 1 Specimen geometry.

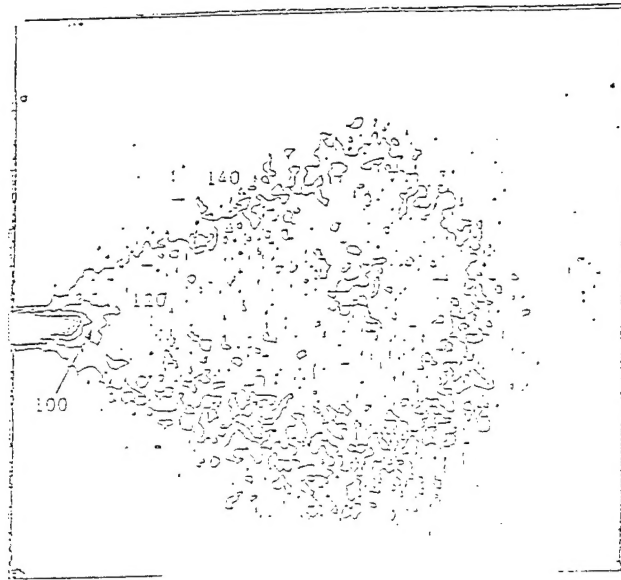


Time= 480 sec

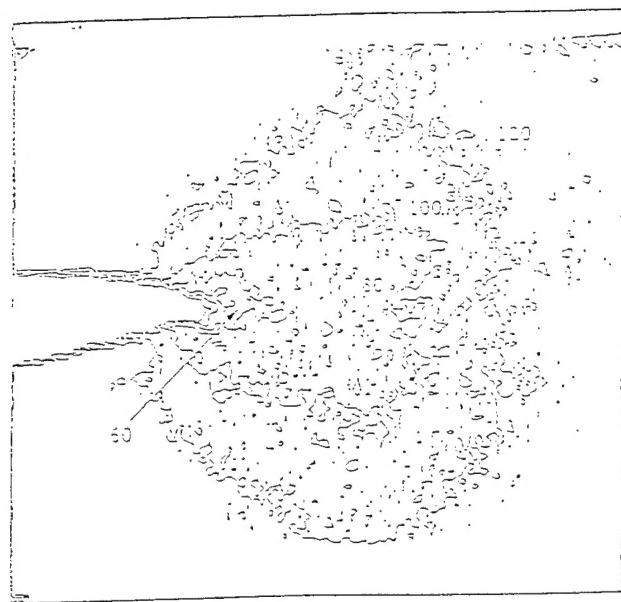


Time=489 sec

Figure 2 Crack opening and growth.



(a) time = 1.6 sec.



(b) time = 5.33 sec.

Figure 3 Iso-intensity contour plots of X-ray image near the crack tip  
( constant strain rate ).

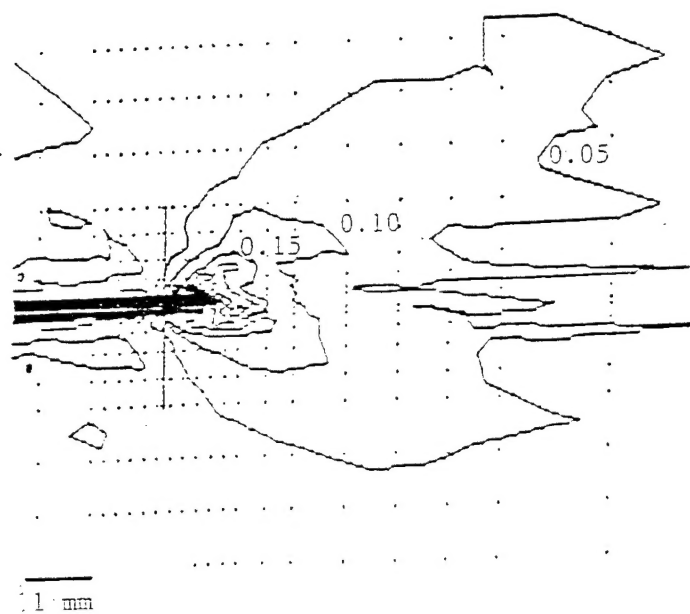


Figure 4 Iso-intensity contour plot normal strain near the crack tip.

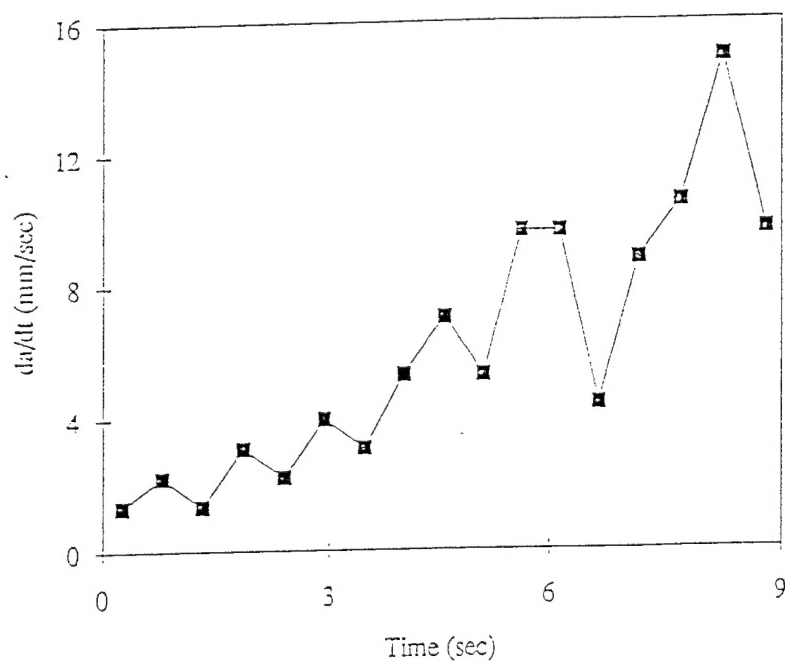
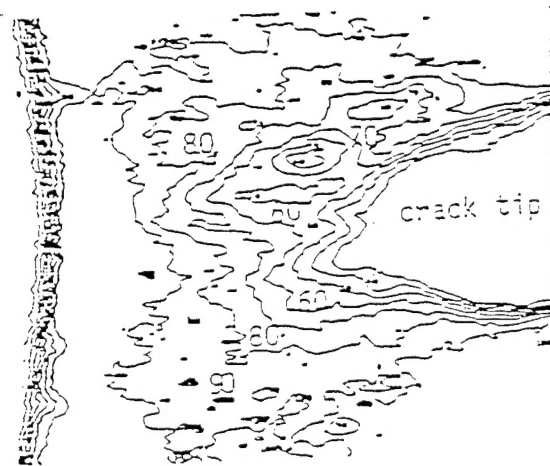
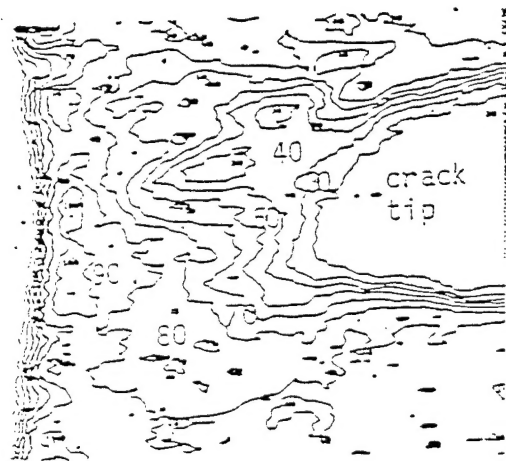


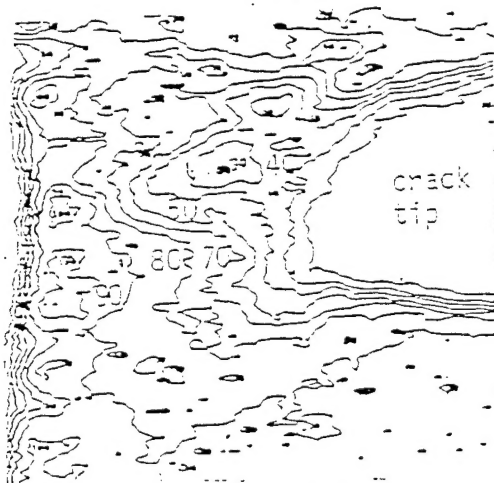
Figure 5 Crack growth rate versus time.



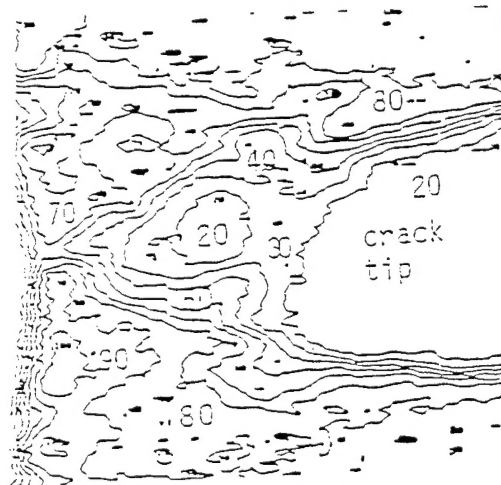
$\epsilon = 13.5\%$



$\epsilon = 13.5\%$

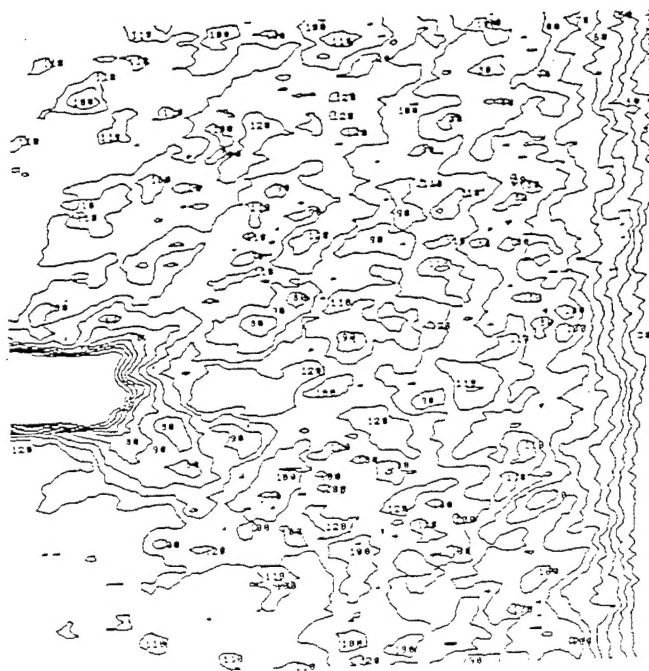


$\epsilon = 13.5\%$

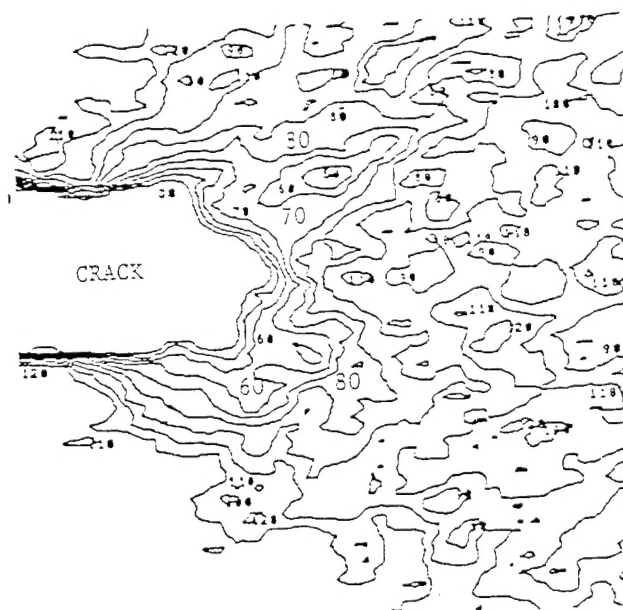


$\epsilon = 13.5\%$

Figure 6 Iso-intensity contour plots of X-ray image near the crack tip  
( constant strain, sharp crack tip ).



$$\epsilon = 3\%$$



$$\epsilon = 6\%$$

Figure 7 Iso-intensity contour plots of X-ray image near the crack tip ( constant strain, blunted crack tip ).